Chalcogenide Letters Vol. 21, No. 9, September 2024, p. 695 - 705

Ab-initio simulation of ferromagnetic chalcogenide $CdCe_2X_4$ (X = S, Se) spinels for optoelectronic applications

M. Zanib[a], M. A. Yasir[a], N. A. Noor[a,*], S. Mumtaz[b],
Mohammad K. Al-Sadoon[c]
[a]*Department of Physics, RIPHAH International University, Campus Lahore, Pakistan*
[b]*Electrical and Biological Physics, Kwangwoon University, Seoul, 01897, South Korea*
[c] *Department of Zoology, College of Science, King Saud University, P.O. Box 2455, Riyadh 11451, Saudi Arabia*

DFT approach was employed to examine the mechanical and optoelectronic properties of $CdCe_2X_4$ (X = S, Se) for investigating their fundamental attributes leading to the FM semiconducting capabilities. In this letter, we computed the precise spin-polarized electrical characteristics using mBJ potential and evaluated the physical and mechanical features via PBEsol-GGA functional. The materials' brittleness has been disclosed by the obtained elastic parameters and related components. According to the analysis of band structure configuration and density of states plots, the aforementioned composites are accounted to be the most durable. In the FM phase, these compounds' durability is because of rare earth Ce ions' exchange splitting within the crystal structure, which is prompted by p-d hybridization. Band exchange splitting has been significantly affected by the participation among impurity cations and resident anions as well as by their spin, charge, and magnetism. In addition, the present study entailed a thorough analysis of the dielectric parameter, which in turn gained insight into the compound's spectral behavior. FM semiconducting features played vital role in scientific improvements of photovoltaic appliances. The parameters estimated in the current investigation might help scientists to explore modifications in the functionality of $CdCe_2X_4$ (X = S, Se).

(Received June 23, 2024; Accepted September 5, 2024)

Keywords: Ferromagnetic spinels, DFT analysis, Magnetic moments, Complex dielectric function, Figure of merit

1. Introduction

Multiple researches have been conducted for the investigations of electromagnetic features of RE based pyrochlores. They are having chemical formula of$vA_2B_2O_7$, in which A stands for +3 cations and B for +4 cations. Although the physical attributes and electro-magnmodes are weakly correlated but an optimal stability is reached by significant changes in magnetic properties, such as magnetic interactions, exchange correlations, and magnetic anisotropy [1–5]. The existence of crystal domains leads to tremendously anisotropic spinning phases, which gives rise to spin freezing attributes in the compounds such as $Ho_2Ti_2O_7$ and $Dy_2Ti_2O_7$. The aforementioned compounds' FM interaction and quantized spinning configurations are similar to those of hexagonal ice patterns [6–13]. There is a geometrical similarity among the spinel sub-lattice (octahedrally aligned ions) and the pyrochlore sub-lattice (lanthanide ions) [14]. On the basis of their complex structural alignment, transition metal (TM) oriented spinel such as $ZnCr_2O_4$ and $CdFe_2O_4$ have drawn a lot of research interest [15]. On the other hand, high spin-lattice interaction in TM oriented spinels provides a viable setting where morphological modifications get entangled with the magnetic configuration [16–17].

* Corresponding author: naveedcssp@gmail.com
https://doi.org/10.15251/CL.2024.219.695

Scholars have performed experiments on the physical and electromagnetic properties of semiconducting spinels, including $CdLn_2Se_4$ (Ln = Dy, Ho) and $CdLn_2S_4$ (Ln = Tm, Ho, Yb, Er) [18, 19]. A combination of NM ions and the scattered floating ions in the crystal structure is accountable for the investigated materials' electromagnetic sub-lattices, which must be comparable to those of pyrochlores. A basic structure similar to pyrochlores has been identified by current investigations of spinel-layered materials such as $CdLn_2S_4$ and $CdLn_2Se_4$, which are marked by architectural complications and have Fd-3m space family. In contrast to rare earth ions, magnetic particles of $CdLn_2(S/Se)_4$ form an alignment of tetrahedron, which were allocated to edges. Interestingly, due to O^{-2} ions' eightfold arrangement, 2.2Å bond length was reported for pyrochlores. Moreover, a spacing of approximately 2.70 Å was also noted for a composition having S-R/Se-R atoms along with a firmly established octahedron [20, 21]. Variation within CEF is caused by ionic arrangements, which created an interesting situation for dimensional information in an enticing context [22]. At 2K, the half-metallic nature in M(B) atoms revealed ice spinning traits in sulphur-based compounds such as $CdEr_2S_4$, a property earlier investigated in $CdEr_2Se_4$ [23]. DFT requires the implementation of adequate exchange-correlation functioning in order to determine the physical and electromagnetic features in magnetic compounds [24]. GMR, TMR and magnetic detection systems were the intriguing advancements of these materials [25]. Previous investigations have raised doubts about the correctness of physical properties of magnetic compounds (as $MgCe_2X_4$ (X = S, Se)) through XC potentials [26, 27]. In order to study the accurate electrical and thermal behavior of $MgCe_2X_4$ (X = S, Se), their dimensional and mechanical properties have been examined via modified gradient approach.

The current study included the investigation of mechanical characteristics of FM semiconducting materials to assess their long-term viability. In order to determine how incoming radiations (with varying frequencies) can affect the electronic characteristics or efficiency of $CdCe_2X_4$ (X = S, Se) spinels, its spectral characteristics were investigated. Properties estimated in the present work will help scientists to discover variations in $CdCe_2X_4$ (X = S, Se) performance in the presence of optical or thermal excitations. This is crucial since FM semiconducting materials are essential for scientific improvements of photovoltaic appliances.

2. Method of calculations

The structural, elastic, spin dependent electronic and optical properties of the concerned compounds $CdCe_2X_4$ (X = S, Se) have been investigated by the implementation of WEIN2k based FP-LAPW technique [28]. Measurements incorporating GGA and mBJ potential were in good agreement with scientific findings [29]. The unit cell's muffin-tin and interstitial sections each have a split spherically symmetric potential which measures energy, electron density, and eigenvalues [30]. In a reciprocal lattice, K_{MAX} represents optimal magnitude of wave vector and the threshold of angular momentum is denoted by lmax and their product is repesented as $R_{MT}\times K_{MAX}$, and have been assigned with values of 10 and 8 correspondingly [31, 32]. 1000 K-points are used in the computation of band structures and optical performance. The conditions for charge and energy convergence are established at 0.00001e and 0.00001 Ry correspondingly.

3. Results and discussion

3.1. Structural and elastic characteristics

The physical investigation of $CdCe_2X_4$ (X = S, Se) provided information about particular ionic locations in the unit cell arrangement, as shown in Fig. 1. The crystalline configuration of $CdCe_2X_4$ (X = S, Se) with Fd-3m (227) space group is accomplished by using the WIEN2K program [28]. Specifically, (0.5, 0, 0), (0.125, 0.125, 0.125) and (0.25, 0.25, 0.25) were the lattice points of Ce, Cd and S/Se atoms respectively. The compound's volume was calculated through Murnaghan model. The respective lattice variables and bulk modulus for $CdCe_2X_4$ (X = S, Se) were found by evaluating their formation energies, as shown in Fig. 2(a, b). The primary measure of the firmness of a substance is its bulk moduli, which express how well a substance can tolerate distortion when

stress is exerted [33, 34]. We examined a_0 and B parameters for $CdCe_2X_4$ (X = S, Se), that are extremely precise compared to already reported composites' experimental and computational findings [35, 36].

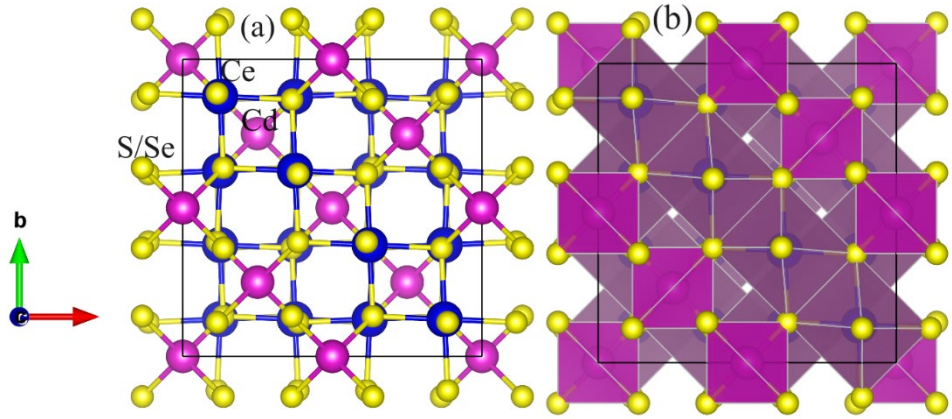

Fig. 1. Unit cell of $CdCe_2X_4$ (X = S, Se) in (a) ball format and (b) polyhedral format, blue, pink, and yellow ball show Ce, Cd, and S/Se atoms respectively.

A crucial tool for determining the fundamental energy and optimal lattice constants is the energy volume optimization curve. The replacement of Se at the S location resulted in a boost of lattice parameters and a drop in bulk modulus. These outcomes confirmed the inverse correlation among lattice constants and bulk moduli. The higher atomic radius of Se has been highlighted by the variation in lattice parameters due to ion replacement. This caused an apparent growth in the crystal lattice [37]. Considering a combination of FM and AFM arrangements inside $CdCe_2X_4$ (X = S, Se) spinels, the spatial distribution of magnetic moments has been described, demonstrating a uniform pattern of both types of spin orientations among the Ce ions. The energy variation between AFM and FM frameworks is represented by the formula $E=E_{FM}-E_{AFM}$. This represents the magnetic connectivity between Ce ions. According to Table 1, the +ve readings of ΔE were determined by using the following formula: $\Delta E=E_{AFM}-E_{FM}$. This demonstrated the greater resilience of concerned compounds in FM phase in contrast to AFM phase (Fig. 2).

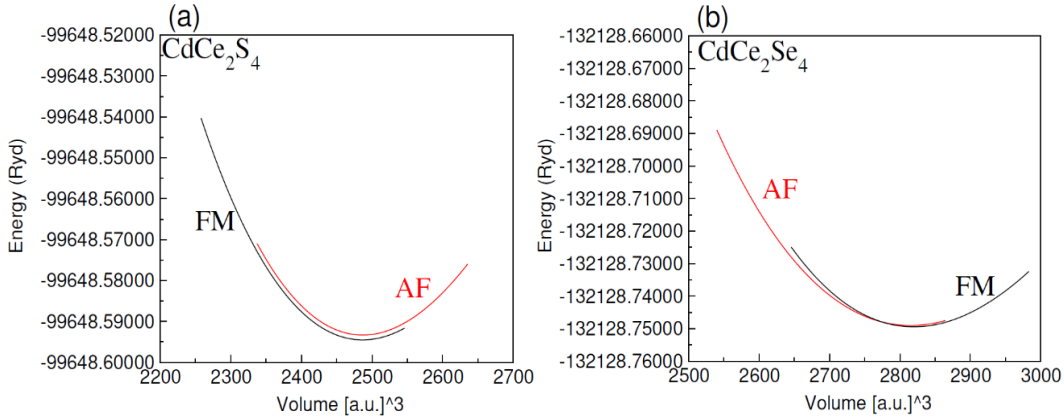

Fig. 2. Volume optimization plot for (a) $CdCe_2S_4$ and (b) $CdCe_2Se_4$ in FM and AFM phases

In the FM state, the long-term viability of the examined composites was confirmed by the determination of –ve ΔH_f values.

$$\Delta H_f = E_{tot}(Cd_lCe_mX_n) - lE_{Cd} - mE_{Ce} - nE_X \quad (1)$$

The material's total energy in its fundamental phase is represented by $E_{tot\ (CdCemXn)}$, while the fundamental energies of the individual particles are indicated by E_{Cd}, E_{Ce}, and E_X. The minus sign associated with the estimated ΔH_f data further supported the thermal durability of the studied material. The aforementioned energy estimations are incorporated to determine ΔH_f.

Table 1. The calculated values of lattice constants, bulk modulus, energy difference (ΔE), and formation energy (ΔH_f (eV)) of chalcogenides $CdCe_2X_4$.

Chalcogenides	a_o(Å)	B_o(GPa)	$\Delta E = E_{AFM}-E_{FM}$	ΔH_f
$CdCe_2S_4$	11.38		8.65	-2.08
$CdCe_2Se_4$	11.86		6.88	-1.88

The computed outcomes demonstrated that the structural configuration is enthusiastically consistent with regard to atomic states. By employing the Charpin approach, C_{11}, C_{12}, and C_{44} were computed [28]. In order to comprehend their functionality, the interaction among structural strain and E_{tot} has been investigated thoroughly. We computed fundamental elastic constants by using given formulas [38-42].

$$B = \frac{1}{3}(C_{11} + 2C_{12}) \quad (2)$$

$$A = \frac{C_{44}}{C_{11}-C_{12}} \quad (3)$$

$$E = \frac{9GB}{3B+G} \quad (4)$$

$$\upsilon = \frac{3B-2G}{2(2B+G)} \quad (5)$$

$$G = \frac{1}{2}(G_v + G_R) \quad (6)$$

$$G_v = \frac{1}{5}(C_{11} - C_{12} + 3C_{44})$$

$$G_R = \frac{5C_{44}(C_{11} - C_{12})}{4C_{44} + 3(C_{11} - C_{12})}$$

The following expression has been utilized for checking the mechanical stability of investigated compounds:

$$C_{11} - C_{12} > 0, C_{11} > 0, C_{44} > 0, C_{11} + 2C_{12} > 0, C_{12} < B < C_{11} \quad (7)$$

The mechanical robustness of $CdCe_2X_4$ (X = S, Se) has been verified by the evaluation of their modulus of elasticity, which have satisfied the above-mentioned relations. Eq. 2 revealed that elastic parameters played a crucial role in the calculation of the Bulk modulus. A significant decline in B_0 values has been observed by the substitution of Se for S, as demonstrated by the reported B measurements (Table 1). Moreover, the compounds also exhibited a significant mechanical anisotropy via Eq. 3. A key indicator of structural rigidity under external stress along specific dimension is Young's modulus (E) (Eq. 4). Data showed that when Se is substituted for S, a substantial decline was observed in G value (Eq. 6). 35.97 GPa and 17.74 GPa are the measured values of G for $CdCe_2S_4$ and $CdCe_2Se_4$ correspondingly. The determined Poisson (υ) and Pugh (B/G) values were less than 0.26 and 1.75, accordingly. On the basis of above-mentioned results, the materials brittle behavior is absorbed. The determined elastic properties indicated that the investigated spinels are appropriate for mechanical applications, regardless of their brittle nature.

Table 2. Calculated elastic constant (C_{11}, C_{12}, C_{44}) and the respective bulk modulus (B), Shear modulus (G), Young Modulus (Y), Poisson's ratio (υ), Pugh ratio ((B_0/G) and anisotropic (A) for chalcogenides $CdCe_2X_4$.

	C_{11}	C_{12}	C_{44}	B_0	G	Y	B_0/G	υ	A
$CdCe_2S_4$	142.81	34.13	27.14	70.35	35.97	92.21	1.95	0.28	0.49
$CdCe_2Se_4$	66.77	55.97	37.07	59.72	17.74	48.43	3.35	0.36	0.85

3.2. Spin-dependent electronic and magnetic characteristic

Fig. 3 demonstrated the spin-oriented band structure (BS) calculations of $CdCe_2X_4$ (X = S, Se) in the FM state by the utilization of optimized lattice parameters. Here, mBJ functional is utilized to verify precision in the band gap calculations. A direct bandgap is formed at the elevated symmetrical spot (Γ) within 1st BZ (referred to Fig 3). The estimated bandgap (E_g) values are 0.9 eV and 0.4 eV for $CdCe_2S_4$ and $CdCe_2Se_4$ respectively. In recognition of IR electromagnetic spectrum, these investigated chalcogenides with these computed E_g values are in great demand in future as similar to Si based narrow bandgap semiconductor [43].

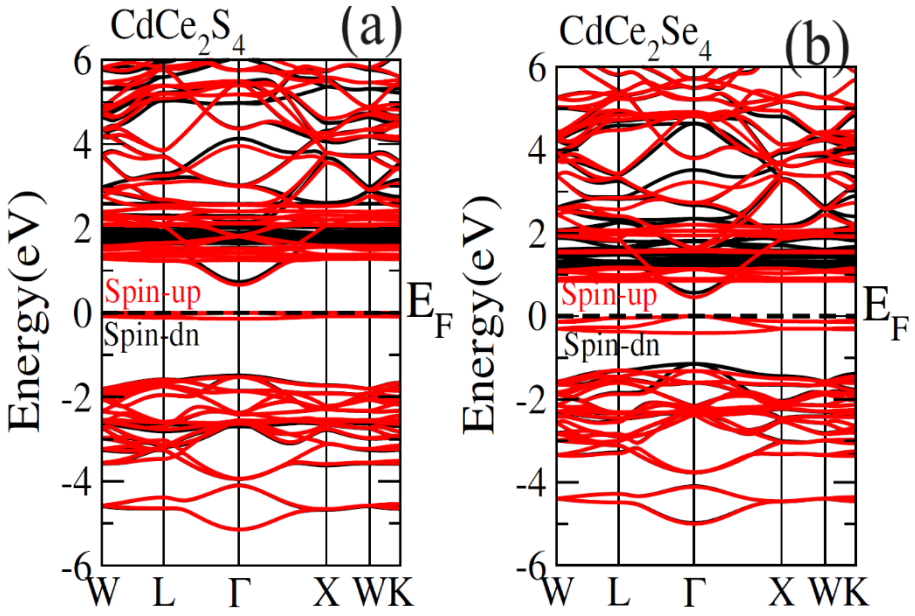

Fig. 3. Spin-dependent electronic band structures of (a) $CdCe_2S_4$ and (b) $CdCe_2Se_4$ f or spin up (red line) spin down (black line).

The partial and total density of states (DOS) plots were determined via mBJ approach. With the spin splitting of rare earth Ce atom in $CdCe_2S_4$ and $CdCe_2Se_4$ framework, several band configurations appear at molecular and orbital levels. In the up-spin channel, CB minima propagate away from the Fermi point due to spin splitting, whereas VB maxima continued to raise to the E_F point. On the other hand, a reverse pattern was observed in the down spin channel. Figs. 4 and 5 illustrated that the PDOS study of individual constituents shed light on FM phenomenon and exchange process. In particular, 5s levels of Cd are located deep in the valence band with energy spectrum (-4 to -6 Ev) and around 3 to 6 eV in the CB spectrum. 4f levels of Ce are found in the CB spectrum between 0 and 3.0 eV. From the Fermi level down to -4 eV, the 3p/4p states of S/Se contributed substantially to VB region.

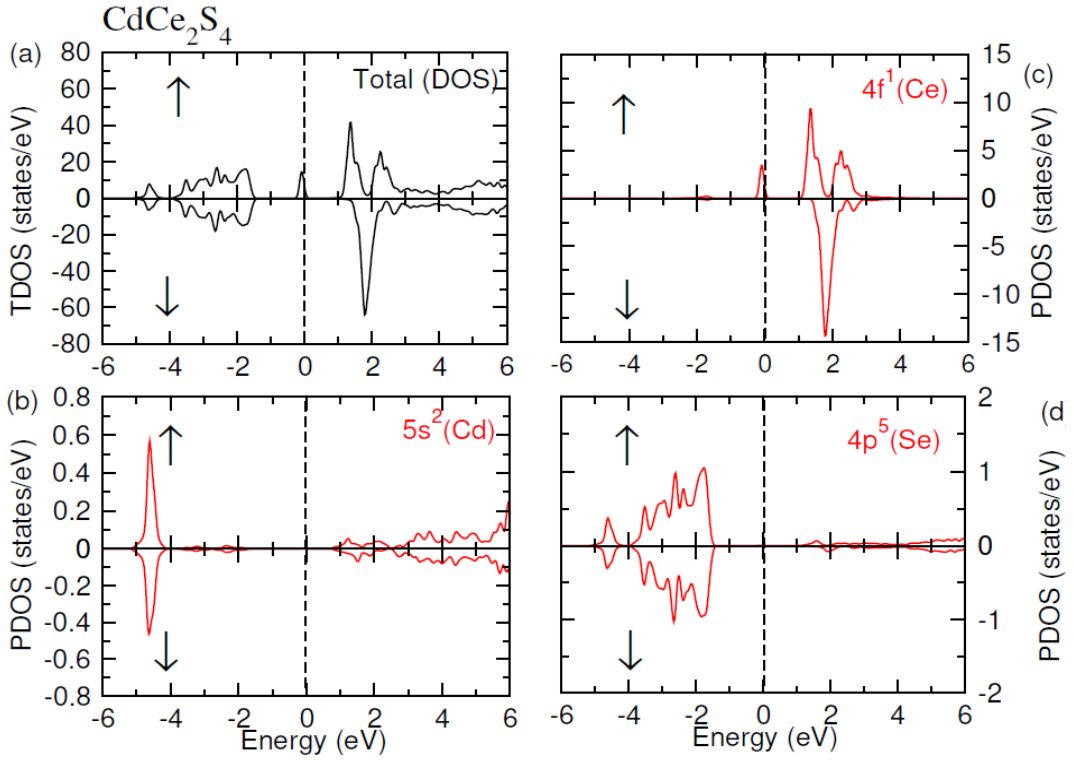

Fig. 4. Density of states plots (TDOS and PDOS) for (a-d) $CdCe_2S_4$ chalcogenide (spin down (↓) and spin up (↑) orientation).

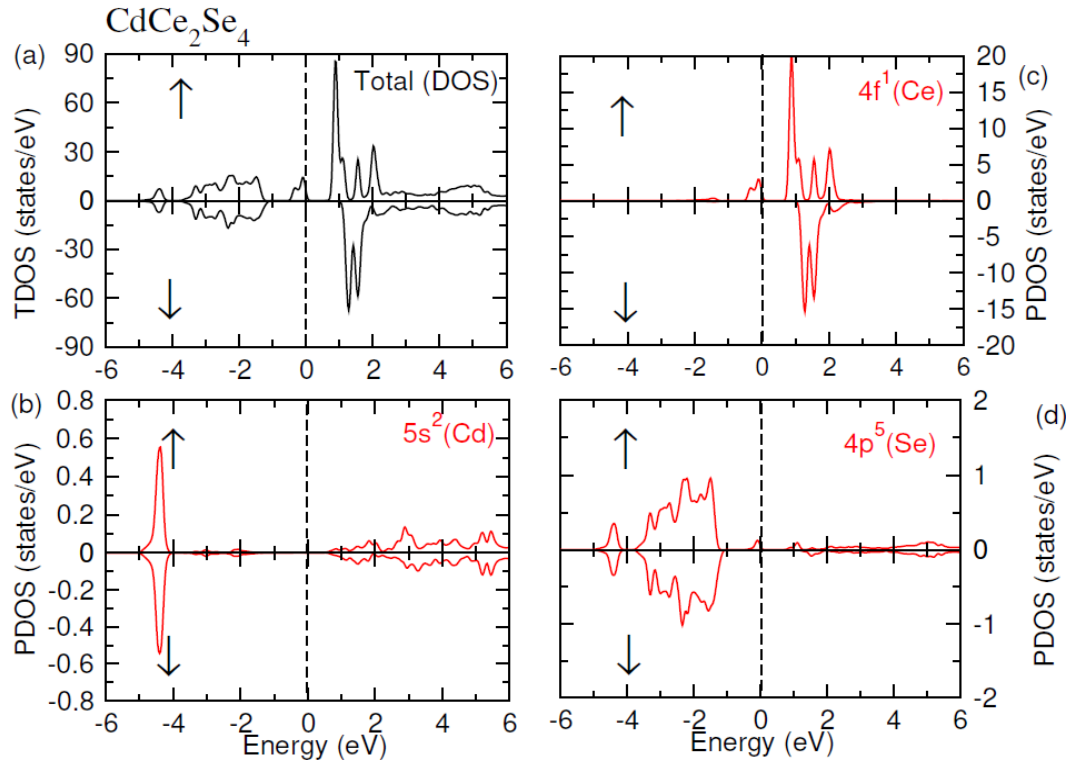

Fig. 4. Density of states plots (TDOS and PDOS) for (a-d) $CdCe_2Se_4$ chalcogenide (spin down (↓) and spin up (↑) orientation).

Table 3 displayed total magnetic moment (TMM) and their local magnetic moment (LMM) values in Bohr magnaton (μ_B). The inclusion of rare earth Ce appeared to greatly improve the total magnetic moment. However, the overall magnetic moment has been substantially affected from Cd and S/Se atoms. As a result, stable ferromagnetic phenomenon has been proven. The computed magnetic moment resulted from the Ce atoms' due to unfilled f orbit, which modifies Ce valence orbit. Substantial exchanges involving the p-subshell of base material and the s-orbits of metals generate μ_B with Zn and S/Se atoms. Due to significant FM exchange dispersion in the studied spinels, Ce displays magnetic-like atomic characteristics. The ferromagnetic feature of the compounds is confirmed by interaction among the S/Se and Cd components.

Table 3. Computed TMM per atom and the LMM (in μ_B) for $CdCe_2S_4$ and $CdCe_2Se_4$.

	Total	M_{Cd}	M_{Cd}	$M_{S/Se}$
$CdCe_2S_4$	2.000	0.001	0.969	0.001
$CdCe_2Se_4$	2.000	0.003	0.942	0.006

3.3. Optical characteristics

The dielectric parameters fully explained the material's spectral properties, which is represented by the formula $\varepsilon(\omega) = \varepsilon_1(\omega)+i\varepsilon_2(\omega)$. Considering 0–10 eV is the energy spectrum in which several spectral parameters were calculated. $\varepsilon_1(\omega)$ explained the phonon scattering whereas its mathematical formula is expressed as [44];

$$\epsilon_1(\omega) = 1 + \frac{2}{\pi} P \int_0^{\infty} \frac{\omega' \epsilon_2(\omega')}{\omega'^2 - \omega^2} d\omega' \tag{8}$$

$$\varepsilon_2(\omega) = \left(\frac{4\pi^2 e^2}{m^2\omega^2}\right) \sum_i^j \int_k < i \vee M \vee j^2 \mathrm{F}_i(1 - \mathrm{F}_i)\delta\left(E_{j,k} - E_{i,k} - \omega\right) d^3k \tag{9}$$

Fig. 6(a) depicted the estimated magnitudes of $\varepsilon_1(0)$ for $CdCe_2X_4$ spinels. 5.40 and 6.8 are the calculated static dielectric parameters of $CdCe_2S_4$ and $CdCe_2Se_4$ respectively. The observed converse relation among $\varepsilon_1(0)$ and E_g was elucidated by Penn's model and expressed as $\varepsilon \propto 1/E_g^2$ [45]. The optimum peak of absorbance is observed at 1.6 eV and 1.1 eV for $CdCe_2S_4$ and $CdCe_2Se_4$ respectively (displayed in Fig. 6(b)). $\varepsilon_2(\omega)$ revealed the absorption properties of investigated composites. A constant growth is observed in the absorbance peak, while exhibiting distinct points corresponding to critical points in the concerned composites. Interestingly, the respective bandgap in the examined materials was found to be inside the IR domain, where notable absorption peaks may be observed. This adjustable bandgap illustrated flexible spectral behavior tailored to specific incoming energy, which in turn indicated their possible uses in photovoltaic and other technological applications. The $n(\omega)$ graphs of investigated materials manifested analogous pattern to that of $\varepsilon_1(\omega)$. The reported readings of n(0) are 2.35 and 2.55 for $CdCe_2S_4$ and $CdCe_2Se_4$ correspondingly, (As shown in Fig. 6(c)). The observed readings of $\varepsilon_1(\omega)$ and $n(\omega)$ comply with the following expression $n^{\wedge 2}$-$k^{\wedge 2}$= $\varepsilon_1(\omega)$ [46].

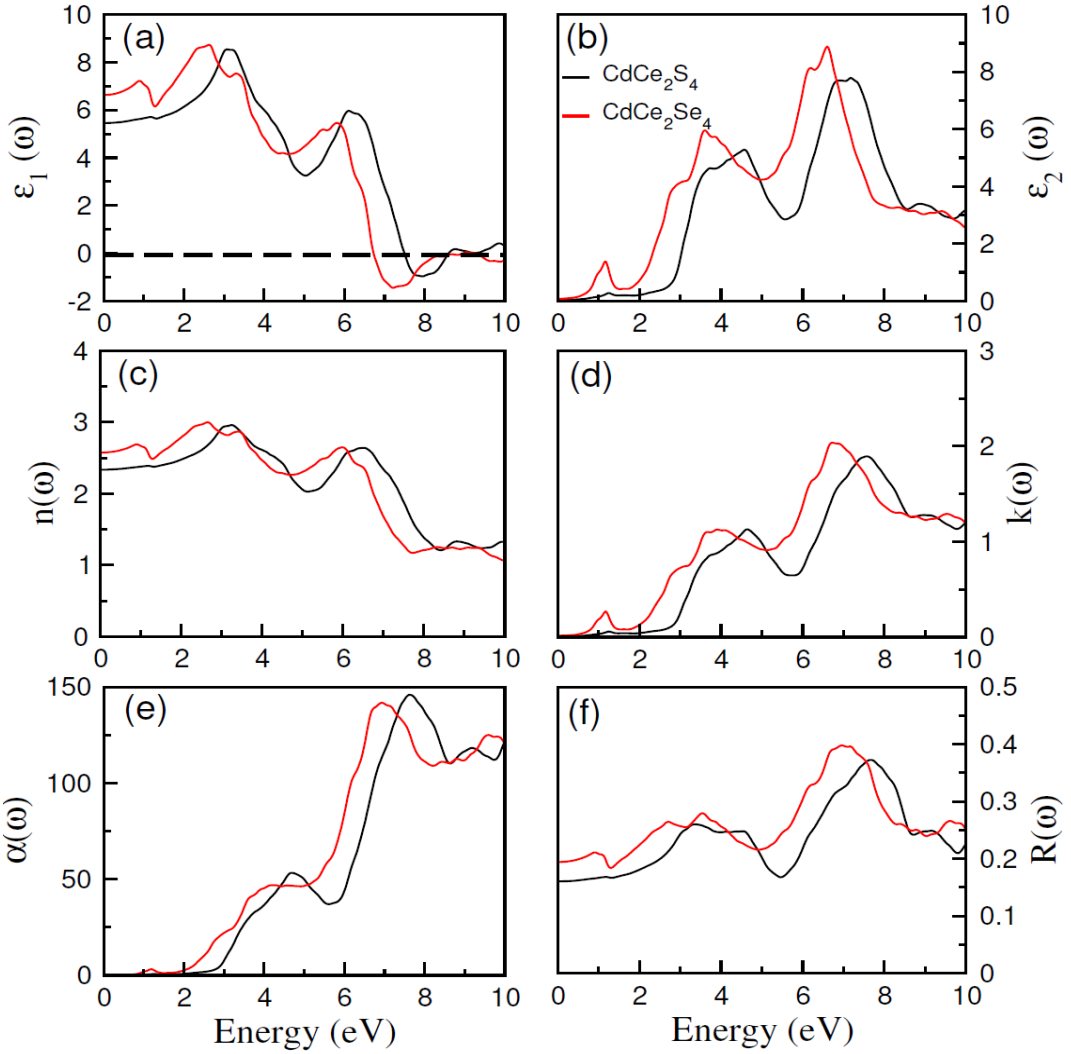

Fig. 6. The computed (a) real part of dielectric $\varepsilon_1(\omega)$, (b) imaginary part of dielectric $\varepsilon_2(\omega)$, (c) refraction $n(\omega)$, (d) extinction coefficient $k(\omega)$, (e) absorption $\alpha(\omega)$, (f) reflectivity $R(\omega)$ for $CdCe_2S_4$ and $CdCe_2Se_4$.

According to Fig. 6(d) illustration, $\alpha(\omega)$, $\varepsilon_2(\omega)$, and $k(\omega)$ executed an analogous pattern. $\alpha=4\pi k/\lambda$ is the equation that is used to compute the coefficient of absorbance (shown in Fig. 6(e)). There is converse relation between absorbance and reflection coefficient. Reflection is an indication of the ability of a substance to bounce the energy which hits off its surface. Here, 0.16 and 0.21 are the estimated R(0) values for $CdCe_2S_4$ and $CdCe_2Se_4$ respectively, (refer to Fig. 6f). Enhanced reflection coefficient is observed in the visible region at around 1 eV, where it approaches approximately 16% and 22% for $CdCe_2S_4$ and $CdCe_2Se_4$ respectively.

4. Conclusion

In the current study, WIEN2k based FP-LAPW approach was employed for the comprehensive analysis of several features of $CdCe_2X_4$ (X = S, Se) chalcogenides. Generalized gradient approach has been utilized for the evaluation of materials' structural and elastic characteristics. Simultaneously, mBJ potential was employed to improve concordance of compounds' electrical and thermoelectric behavior with experimental results. The spinels' durability was confirmed by the calculated formation energy in FM phase. Whereas their fundamental energies in the AFM phases were smaller than those in FM phases. Additionally, both spinels satisfy elastic

endurance requirements, demonstrating their mechanical durability. The noteworthy hybridization and XC phenomenon in the concerned compounds highlighted the significance of spinning trait in FM phenomenon, having TMM equal to $2\mu_B$. The aforementioned materials' direct bandgap semiconducting feature has been demonstrated by computation of their electrical characteristics. Furthermore, the mechanical characteristics indicated their possible applications in mechanical systems. The optical features shed light on how highly energized incident photons can affect the electronic characteristics and functionality of the FM semiconductor $CdCe_2X_4$ (X = S, Se).

Funding

Researchers Supporting Project number (RSP2024R410), King Saud University

Acknowledgements

We extend our appreciation to the Researchers Supporting Project (RSP2024R410), King Saud University, Riyadh, Saudi Arabia.

References

[1] J. D. M. Champion, M. J. Harris, P. C. W. Holdsworth, A. S.Wills, G. Balakrishnan, S. T. Bramwell, E. Cizmar, T. Fennell, J.S. Gardner, J. Lago, D. F. McMorrow, M. Orendac, A. Orendacova,D. McK. Paul, R. I. Smith, M. T. F. Telling, A.Wildes, Phys. Rev. B 68, 02040 (R) (2003).

[2] M. J. P. Gingras, C. V. Stager, N. P. Raju, B. D. Gaulin, and J. E.Greedan, Phys. Rev. Lett. 78, 947(1997); https://doi.org/10.1103/PhysRevLett.78.947

[3] Y.L. Aung, A. Ikesue, R. Yasuhara, Y. Iwamoto, J. Alloys Compd. 822 (2020) 153564; https://doi.org/10.1016/j.jallcom.2019.153564

[4] A. Panghal, Y. Kumar, P.K. Kulriya, P.M. Shirage, N.L. Singh, J. Alloys Compd. 862 (2021) 158556; https://doi.org/10.1016/j.jallcom.2020.158556

[5] J. S. Gardner, S. R. Dunsiger, B. D. Gaulin, M. J. P. Gingras, J. E.Greedan, R. F. Kiefl, M. D. Lumsden, W. A. MacFarlane, N. P.Raju, J. E. Sonier, I. Swainson, Z. Tun, Phys. Rev. Lett. 82,1012 (1999).

[6] G.V. Bazuev, T.I. Chupakhina, A.V. Korolyov, J. Alloys Compd. 486 (2009) 88-92; https://doi.org/10.1016/j.jallcom.2009.07.021

[7] S. T. Bramwell, M. J. Harris, J. Phys.: Condens. Matter 10 (1998) L215; https://doi.org/10.1088/0953-8984/10/14/002

[8] A. P. Ramirez, A. Hayashi, R. J. Cava, R. Siddharthan, B. S.Shastry, Nature (London) 399 (1999) 333; https://doi.org/10.1038/20619

[9] J. Snyder, J. S. Slusky, R. J. Cava, P. Schiffer, Nature London 413 (2001) 48; https://doi.org/10.1038/35092516

[10] J. Snyder, B. G. Ueland, A. Mizel, J. S. Slusky, H. Karunadasa, R. J. Cava, P. Schiffer, Phys. Rev. B 70 (2004) 184431.

[11] J. Snyder, B. G. Ueland, J. S. Slusky, H. Karunadasa, R. J. Cava, P. Schiffer, Phys. Rev. B 69 (2004) 064414.

[12] H. Fukazawa, R. G. Melko, R. Higashinaka, Y. Maeno, M. J.P. Gingras, Phys. Rev. B 65 (2002) 054410; https://doi.org/10.1103/PhysRevB.65.054410

[13] J. Snyder, B. G. Ueland, J. S. Slusky, H. Karunadasa, R. J. Cava,A. Mizel, P. Schiffer, Phys. Rev. Lett. 91 (2003) 107201.

[14] H. Martinho, N. O. Moreno, J. A. Sanjurjo, C. Rettori, A. J.Garcia-Adeva, D. L. Huber, S. B. Oseroff, W. Ratcliff II, S. W.Cheong, P. G. Pagliuso, J. L. Sarrao, G. B. Martins, Phys.Rev. B 64 (2001) 024408

[15] J. Ostorero, A. Mauger, M. Guillot, A. Derory, M. Escorne, A. Marchand, Phys. Rev. B 40 (1989) 391; https://doi.org/10.1103/PhysRevB.40.391

[16] L. Morellon, P. A. Algarabel, M. R. Ibarra, J. Blasco, B. Garcia-Landa, Z. Arnold, F. Albertini, Phys. Rev. B 58 (1998) R14721;

[17] W. Choe, V. K. Pecharsky, A. O. Pecharsky, K. A. Gschneidner,V. G. Young, G. J. Miller, Phys. Rev. Lett. 84 (2000) 4617; https://doi.org/10.1103/PhysRevLett.84.4617

[18] O. M. Aliev, A. B. Agaev, and R. A. Azadaliev, Inorg. Mater. 33 (1997) 1123.

[19] G. C. Lau, R. S. Freitas, B. G. Ueland, P. Schiffer, R. J. Cava, Phys. Rev. B 72, (2005) 054411; https://doi.org/10.1103/PhysRevB.72.054411

[20] G. C. Lau, R. S. Freitas, B. G. Ueland, P. Schiffer, R. J. Cava, Phys.Rev. B 72, (2005) 054411; https://doi.org/10.1103/PhysRevB.72.054411

[21] O. Knop, F. Brisse, L. Castelli, R. Sutarno, Can. J. Chem. 43 (1965) 2812; https://doi.org/10.1139/v65-392

[22] J. Lago, I. Zivkovic, B. Z. Malkin, J. Rodriguez Fernandez, P. Ghigna, P.Dalmas de Reotier, A. Yaouanc, T. Rojo, Phys. Rev. Lett. 104 (2010) 247203; https://doi.org/10.1103/PhysRevLett.104.247203

[23] L. Ben-Dor, I. Shilo, J. Solid State Chem. 35 (1980) 278; https://doi.org/10.1016/0022-4596(80)90504-6

[24] S.K. Pandey, Phys. Rev. B. 86 (2012) 085103; https://doi.org/10.1103/PhysRevB.86.085103

[25] F. Estrada, E.J. Guzmán, O. Navarro, M. Avignon, Phys. Rev. B. 97 (2018) 195155; https://doi.org/10.1103/PhysRevB.97.195155

[26] S.M. Thompson, J. Phys. D: Appl. Phys. 41 (2008) 093001; https://doi.org/10.1088/0022-3727/41/9/093001

[27] A. Jain, S. P. Ong, G. Hautier, W. Chen, W. D. Richards, S. Dacek, S. Cholia, D. Gunter, D. Skinner, G. Ceder, K. A. Persson, APL Materials, 1 (2013), 011002; https://doi.org/10.1063/1.4812323

[28] P. Blaha, K. Schwarz, G. Madsen, D. Kvasnicka, J. Luitz , An augmented plane wave plus local orbital program for calculating crystal properties. Vienna University of Technology, Vienna, Austria. 2001

[29] Z. Wu, E. R. Cohen, Phys. Rev. B 73 (2006)235116; https://doi.org/10.1103/PhysRevB.73.235116

[30] F. Tran, P. Blaha, Phys. Rev. Lett. 102 (2009) 226401; https://doi.org/10.1103/PhysRevLett.102.226401

[31] Q. Mahmood, S.M. Alay-e-Abbas, M. Hassan, N.A. Noor, J. Alloys Compd. 688 (2016) 899-907; https://doi.org/10.1016/j.jallcom.2016.07.302

[32] G.K. Madsen, D.J. Singh, Comput. Phys. Commun. 175 (2006) 67; https://doi.org/10.1016/j.cpc.2006.03.007

[33] M. I. Aroyo, A. Kirov, C. Capillas, J. M. Perez-Mato, H. Wondratschek, Acta Cryst. A62 (2006) 115-128; https://doi.org/10.1107/S0108767305040286

[34] F. Murnaghan. Proc. National Acad. Sci. 30(1944) 244-247; https://doi.org/10.1073/pnas.30.9.244

[35] L Ben-Dor, I Shilo, Solid State Chem. 35 (1980) 278; https://doi.org/10.1016/0022-4596(80)90504-6

[36] GC Lau, RS Freitas, BG Ueland, P Schiffer, RJ Cava - Physical Review B,72(2005), 054411; https://doi.org/10.1103/PhysRevB.72.054411

[37] S. D. Reddy, M. Reddy, N. Raok, K. Gunasekhar, S. P. Reddy, J. Opt. Adv. Mater. 9 (2007) 3743-3746

[38] X. Ji, Y. Yu, J. Ji, J. Long, J. Chen, D. Liu, J. Alloy. Compd. 623 (2015) 304-310; https://doi.org/10.1016/j.jallcom.2014.10.151

[39] V. Tvergaard, J.W. Hutshinson, J. Am. Ceram. Soc. 71 (1988) 157-166. https://doi.org/10.1111/j.1151-2916.1988.tb05022.x

[40] S.F. Pugh, Philos. Mag. 45 (1954) 823-843; https://doi.org/10.1080/14786440808520496

[41] L. Kleinman, Phys. Rev. 128 (1962) 2614-2621; https://doi.org/10.1103/PhysRev.128.2614

[42] M.B. Kanoun, A.E. Merad, J. Cibert, H. Aourag, G. Merad, J. Alloy. Compd. 366(2004) 86-93; https://doi.org/10.1016/j.jallcom.2003.07.005

[43] Wong, Joeson, Stefan T. Omelchenko, and Harry A. Atwater, ACS Energy Letters 6 (2020) 52-57; https://doi.org/10.1021/acsenergylett.0c02362

[44] M Robail, NA Noor, MW Iqbal, H Ullah, A Mahmood, M. A. Naeem, Y. H. Shin, Ceramics International, 48 (2022), 2385-2393; https://doi.org/10.1016/j.ceramint.2021.10.019

[45] D.R. Penn, Physical Review, 128 (1962) 2093; https://doi.org/10.1103/PhysRev.128.2093

[46] M Hassan, I Arshad, Q Mahmood, Semicond. Sci. Technol.32 (2017) 115002; https://doi.org/10.1088/1361-6641/aa8afe